High temperature self-assembly of Ag nanowires on vicinal Si(001)

2005 J. Phys.: Condens. Matter 17 S1407

(http://iopscience.iop.org/0953-8984/17/16/011)

INSTITUTE OF PHYSICS PUBLISHING JOURNAL OF PHYSICS: CONDENSED MATTER

J. Phys.: Condens. Matter **17** (2005) S1407–S1414 doi:10.1088/0953-8984/17/16/011

High temperature self-assembly of Ag nanowires on vicinal Si(001)

K R Roos[1], K L Roos[2], M Horn-von Hoegen[3] and F-J Meyer zu Heringdorf[3]

[1] Department of Physics, Bradley University, Peoria, IL 61625, USA
[2] Department of Materials Science and Engineering and Materials Research Laboratory, University of Illinois at Urbana-Champaign, Urbana, IL 61801, USA
[3] Institut für Laser-und Plasmaphysik, Universität Duisburg-Essen, 45117 Essen, Germany

Received 9 December 2004, in final form 9 December 2004
Published 8 April 2005
Online at stacks.iop.org/JPhysCM/17/S1407

Abstract

We have used low energy electron microscopy (LEEM) and photo emission electron microscopy (PEEM) to study the high temperature (620 °C) self-assembly of Ag nanowires on vicinal Si(001), miscut 4° in the [110] direction. After formation of an initial wetting layer, growth of wire-like structures proceeds with subsequent deposition. Simultaneously, compact islands form and the nanowires comprise only a minority of the total Ag deposit. The wires display quasi-one-dimensional behaviour as their length is observed to increase while their width remains constant. The lengths of the wires can be controlled and we have routinely grown wires longer than 100 μm. A kinetically limiting process, wherein mass transport is suppressed in the direction normal to the direction of elongation, is identified as a contributor to the growth of the nanowires.

1. Introduction

During epitaxial growth, anisotropic surfaces typically transmit their anisotropic characteristics to the growing adlayers. This can lead to the phenomenon of self-assembly wherein the substrate surface acts as a template for forming the depositing material into nanostructures which are scientifically and technologically interesting. The self-assembly of elongated metallic islands (or nanowires) on semiconductor surfaces is of particular interest technologically because of their potential for use as interconnects in electronic devices, and scientifically, since they provide a subject for the study of the physics of formation of quasi-one-dimensional systems.

There have been only a few studies of the self-assembly of nanowires on Si surfaces with low energy electron microscopy (LEEM). Tersoff and Tromp [1] observed the formation of elongated Ag islands on bare Si(100), and presented a model which predicts a shape transition of the Ag islands from compact to elongated based on a thermodynamic model. The model

assumes that the misfit strain plays the dominant role in forming the wire-shaped islands. However, high resolution transmission electron microscopy and LEEM studies [2] of the growth and decay of Ag nanowires on the hydrogen-terminated Si(001) surface reveal two important observations:

(i) that the misfit between the epitaxial Ag(001) layers of the nanowires and the Si(001) substrate is only 0.3%, and
(ii) that the elongated shape of the Ag nanowires may not be energetically favourable.

These observations question the role that misfit strain plays in forming the elongated structures.

Jalochowski and Bauer [3, 4] formed similar nanowires of Pb on different Si substrates by depositing Pb near room temperature, and subsequently annealing to higher temperatures. An important step in the Pb wire study was the controlled pre-faceting of the Si surfaces before Pb deposition. The faceting was accomplished by depositing a submonolayer of Au at RT, and then annealing to high temperature. This Au-induced modification process creates quasi-one-dimensional facets and superstructures [3, 4]. For the special case of the vicinal Si(001) surface, miscut 4° in the [110] direction, the Au-modification process causes the surface to reconstruct into flat (001) terraces [5] separated by step-bunches that thermodynamically favour a well defined facet [6–8]. The formation mechanism for the Pb nanowires was attributed [3, 4] to lattice mismatch strain, one-dimensional diffusion, and a further anisotropic component due to the Au-induced superstructure on the terraces.

In this paper we present LEEM and photo-emission electron microscopy (PEEM) studies of the controlled growth of Ag nanowires on vicinal Si(001), miscut 4° in the [110] direction, and identify a kinetic mechanism that could account for the late stage nanowire growth. We use the term 'nanowire' in reference to the elongated islands we observe as growth at relatively low temperatures produces nanoscopic wire widths. However, at the high temperatures and growth times we report in this paper the wire widths can become *micro*scopic. Whereas the Pb nanowires [3, 4] were formed on Au-modified Si via the combination of low temperature growth and high temperature annealing, in our study we grow Ag on the bare Si surface at elevated temperature to minimize kinetic limitations. While we have also studied the growth of Ag nanowires on the Au-faceted surface [9], here we only concentrate on the much simpler system of Ag/Si(001).

2. Experimental setup

The experimental LEEM and PEEM observations were made using IBM's UHV LEEM-I prototype [10], now located at the University of Duisburg-Essen. The PEEM images were recorded by illuminating the sample with UV light from a standard Hg discharge lamp. The Si samples were cut from high-resistivity, 4° vicinal Si wafers from Silizium Bearbeitung Andrea Holm, Germany. The samples were heated by electron bombardment from a filament mounted behind the sample. New samples were typically outgassed for several hours at 700 °C, and were then repeatedly flashed to 1250 °C to remove the native oxide. The last step in producing a well ordered surface was slow cooling to the deposition temperature. The temperature of the sample was measured by an IR-pyrometer with emissivity corrections. Ag desorbs from the Si(001) surface at the elevated temperatures used in this study so the desorption must be sufficiently compensated with the Ag deposition flux to produce dynamic growth on the surface. Ag was evaporated from a resistively heated quartz crucible at a constant rate of 1 ML per 120 s of deposition time for all the growth experiments described herein. The rate was calibrated inside the microscope using the known saturation coverage [11] for the $(\sqrt{3} \times \sqrt{3})$-R30° reconstruction of Ag on Si(111)-(7 × 7).

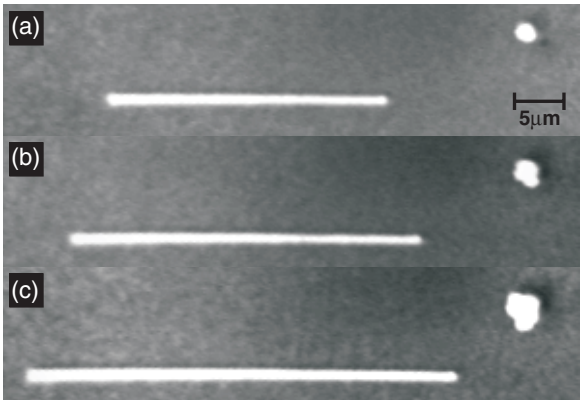

Figure 1. PEEM images of a wire-like Ag island and a compact island during growth on vicinal Si(001) at 620 °C for Ag deposition times of (a) 16 min, (b) 22 min and (c) 32 min.

3. Experimental results

The vicinal substrate was miscut 4° from the (001) plane in the [110] direction. This double-stepped surface consists only of type-D_B [12] steps with uniform terrace widths of roughly 36 Å [13], and only one of the two possible Si(001)-(2 × 1) reconstructed domains is present on the surface. The dimer rows align in a direction perpendicular to the steps separating the terraces. This vicinal Si(001) surface imaged in PEEM appears dark and featureless as the narrow terraces cannot be resolved. At a deposition temperature of 620 °C the first 0.5 ML of Ag goes down as a (2 × 3)-Ag wetting layer. This overlayer has a coverage of 1 ML with respect to the underlying Si(001)-(1 × 2), and thus includes 0.5 ML of Si atoms from the substrate [14, 15]. During the formation of the Ag wetting layer the PEEM image brightens considerably due to the difference in electronic structure between the bare Si surface and the (2 × 3)Ag overlayer. The first resolvable features in PEEM are bright Ag islands that begin to appear shortly after the (2 × 3)Ag overlayer is complete. A small minority of these bright Ag islands can be readily identified as elongated wire-like islands, while most of the islands are compact. At these growth conditions (Ag deposition flux = (1/120) ML s^{-1} and sample temperature = 620 °C) the density of the elongated islands is so low that it is extremely unlikely that the initial 100 μm field of view will contain one. It is thus typically necessary to step around the surface until one of the nanowires is found, making it practically impossible to study the initial nucleation of a wire.

Shown in figure 1 is a series of PEEM images at different times during growth of Ag after one of the nanowires has been located and moved into the field of view. Clearly, the width of the wire does not increase while the length does. In figure 1(c) the wire has reached a length of ∼44 μm; however, we have routinely observed such wires grow to lengths of more than 100 μm. Analysis of LEEM images of the wires and the associated microdiffraction patterns reveals that the nanowires grow lengthwise parallel to the double steps; that is, in the $[\bar{1}10]$ direction. The compact Ag island in figure 1 coarsens during the lengthening of the nanowire, and grows three-dimensionally.

Figures 2(a) and (b) show different regions of the surface after an Ag deposition time of 40 min displaying two nanowires with very high aspect ratios. Interestingly, in figure 2(b) a 'collision event', indicated by the dark arrow, has occurred between a growing nanowire and a compact island, fixing the position of this end of the wire. The united entity remains

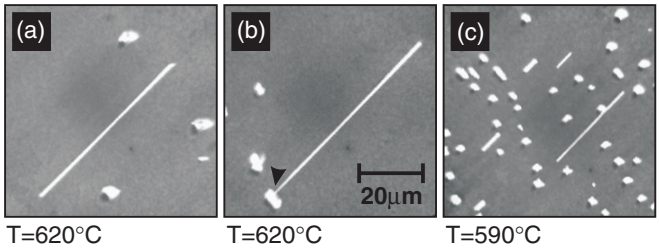

Figure 2. (a) PEEM image of a long Ag nanowire grown on vicinal Si(001) at 620 °C. The total Ag deposition time was 40 min. (b) A different Ag nanowire grown under the same conditions as in (a). The dark arrow indicates the point where the long wire has coalesced with a compact island (see the text). (c) PEEM image of Ag nanowires and compact islands after an Ag deposition time of 40 min at 590 °C.

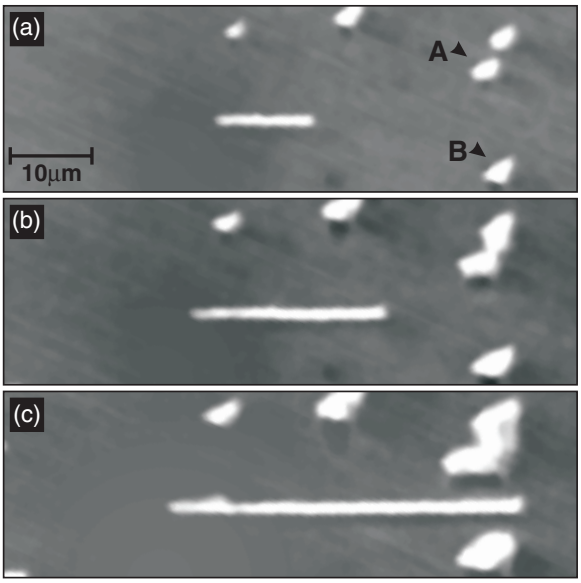

Figure 3. PEEM images of a long Ag nanowire during growth at 620 °C for Ag deposition times of (a) 6 min, (b) 26 min, and (c) 90 min. The wire approaches (b), and eventually passes between (c), the two compact islands labelled A and B in (a).

stable, however, and does not collapse into a compact island, suggesting that despite the high temperature the growth of the wire is kinetically limited. The effect of depositing Ag at a lower substrate temperature can be seen by comparing figures 2(a) and (b) with figure 2(c), which shows the surface after a deposition time of 40 min at 590 °C. The same deposition flux of (1/120) ML s^{-1} was used for figure 2(c). The lower deposition temperature produces a higher density of (shorter) wires and compact islands, as expected from classical nucleation theory [16] since the lower substrate temperature produces a lower ratio of the surface diffusion coefficient to deposition flux, D/F.

Figure 3 shows PEEM images of a nanowire grown at 620 °C for different Ag deposition times. As its length increases the right end of the wire approaches a region flanked by two marked Ag islands. The right end of the wire grows more quickly than the left end, and eventually the left end becomes pinned, perhaps by the presence of some defect. Figure 3(a)

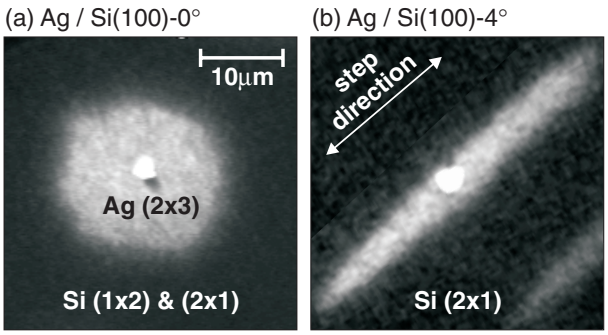

Figure 4. PEEM images of an Ag island and surrounding (2 × 3)Ag iso-coverage zones taken during desorption at 670 °C from (a) flat Si(001), and (b) from vicinal 4° Si(001). For the vicinal surface the step direction is indicated in the upper left.

shows the wire's position when it was first observed, figure 3(b) shows it when its right end has been extended to a position roughly half-way between its initial position and the middle region between the two compact islands, and figure 3(c) shows the wire after it has passed the two islands. From a simplistic point of view this seems surprising since the existence of capture zones around the marked islands should prevent additional Ag from reaching the end of the wire.

To understand why the island passes through the two-island 'gate', it is helpful to analyse the diffusion of the Ag in more detail. At high temperature, where desorption of Ag from the surface takes place, it is known from Auger investigations [17] that while Ag desorbs from the areas between the islands, the Ag islands feed Ag adatoms onto the surface in an attempt to keep the surface covered with Ag. Thus, if the effective diffusion length is less than the average island separation, isolated regions of higher Ag coverage will form around each island. Shown in figure 4 are PEEM images of Ag islands and their immediate surroundings taken during desorption of Ag from the surface at 670 °C without Ag deposition. Figure 4(a) shows an Ag island decaying on a flat Si(001) surface, and figure 4(b) shows an Ag island decaying on a 4° vicinal Si(001) surface. In each, a bright Ag island is seen in the middle of a grey region that forms an abrupt boundary with the rest of the surface that appears dark. Microdiffraction reveals that dark areas correspond to (2 × 1) reconstructed Si(001) areas, while the grey zone around the island displays a (2 × 3)Ag reconstruction. In figure 4(b) only one of the two possible Si(001)-(2 × 1) domains is seen in the microdiffraction pattern of the dark part of the surface, as expected for a surface with only D_B-type steps. Also in figure 4(b) the microdiffraction pattern of the grey region between the island and the dark surface shows only one domain of the (2 × 3)Ag reconstruction. However, two equivalent Si(001)-(2 × 1) and (2 × 3)-Ag domains, rotated by 90°, are observed in the respective regions for the flat Si(001) surface of figure 4(a). The contrast between the bright and dark areas in the images is due to the difference in the electronic structure between the bare Si (dark), the (2 × 3)-Ag region (grey), and the Ag island (bright).

The grey region around the island with the (2 × 3)Ag reconstruction corresponds to an area which can be sampled by the Ag adatoms leaving the decaying Ag island; thus, it is a direct image of regions of more or less constant saturation coverage surrounding the islands. We refer to these constant coverage regions as 'iso-coverage zones'. Although in figure 4 the iso-coverage zones are only shown for the compact islands, the iso-coverage zones surrounding the wires display shapes similar to those surrounding the compact islands on their respective surfaces. From the shape of the iso-coverage zone in figure 4(a) we conclude that diffusion

of Ag adatoms on the (2 × 3)Ag reconstructed surface on non-vicinal Si(001) is effectively isotropic. The striking feature in figure 4 is the anisotropic shape of the iso-coverage zone for the vicinal Si(001) surface of figure 4(b). While it is elongated in the direction of growth of the wires along the step edges of the Si substrate, it is also contracted in the direction perpendicular to the steps. We attribute this anisotropic diffusion to the presence of a barrier to interlayer diffusion at the steps on this surface which run parallel to the growing wires. Since the experiment in figure 3 was performed on a miscut surface similar to figure 4(b), the capture zones around the islands, labelled A and B in figure 3, are expected to have a shape similar to the iso-coverage zone in figure 4(b). Thus, the wire growing through the gate of figure 4 must be due to little or no influence from the Ag adatoms' capture zones of the compact islands. It further demonstrates the quasi-one-dimensional nature of the surface: in particular, that surface diffusion of Ag adatoms is suppressed in the [110] direction (perpendicular to the wires) on the vicinal surface.

4. Discussion and conclusion

From the present data we believe that the observed highly anisotropic surface diffusion in this system is the key factor to the growth of the nanowires. After the formation of the wetting layer on vicinal Si(001), subsequent growth occurs on top of the (2 × 3)Ag surface. For the underlying Si substrate, it is known from diffusion studies on Ge(001) and Si(001) [18, 19] that the diffusion of ad-dimers along the dimer rows is much faster than the diffusion across the dimer rows. The structure for (2 × 3)-Ag has been described [14] as Ag-decorated rows of Si atoms, suggesting that the anisotropic nature of the diffusion of the underlying Si(001) surface is maintained in the (2 × 3)-Ag. For our vicinal substrate, this fast diffusion direction would be perpendicular to the step edges. For wires to extend along the step edges, i.e. preferentially grow in the slow diffusion direction, some mechanism must act to suppress the adatom diffusion in the direction perpendicular to the growing wire, thus effectively turning the slow diffusion direction into the fast one.

The key to understanding the suppression of the surface diffusion in the fast direction may be the identification of a barrier to mass transport into the sides of the growing wires. Agglomerations of steps into step-bunches may act as such a barrier. It has been observed with SPA-LEED [20] that deposition of Ag on the 4° vicinal Si(001) at the same temperature (620 °C) used in our study causes the surface to rearrange into a hill-and-valley structure composed of flat (001) terraces bounded by six-fold step-bunches. We also observe this step-bunching. Shown in figure 5 are reciprocal space maps [21, 22] of the reciprocal lattice of the surface in the [110] direction obtained by LEEM. This direction allows us to directly image the reciprocal lattice rods from both the step-bunches in the Si and the side facets of the Ag-wires. Both figures 5(a) and (b) display a similar section of reciprocal space with an electron energy range between 0 and ∼20 eV, corresponding to a scattering phase range of $S = 0$ to $S \sim 1$ [21]. Figure 5(a) was produced from a microdiffraction pattern of a region of the substrate between growing wires during Ag deposition at high temperature. The central vertical (00) rod and the half-integer order rods of the (2 × 3)Ag are clearly visible. In addition, weak, slanted rods are indicative of a system of poorly ordered (115) facets on the surface. The wires are thus formed on a surface containing step-bunches. Figure 5(b) was produced from a microdiffraction pattern formed with a segment of a growing wire directly positioned in the centre of the electron beam. The reciprocal space maps for compact islands centred in the electron beam are similar to those for the nanowires. The pattern in (b) appears distorted compared to (a) simply because the three-dimensional shape of the wire affects the imaging of the diffraction plane in the LEEM. The signature of the step-bunches from figure 5(a), though

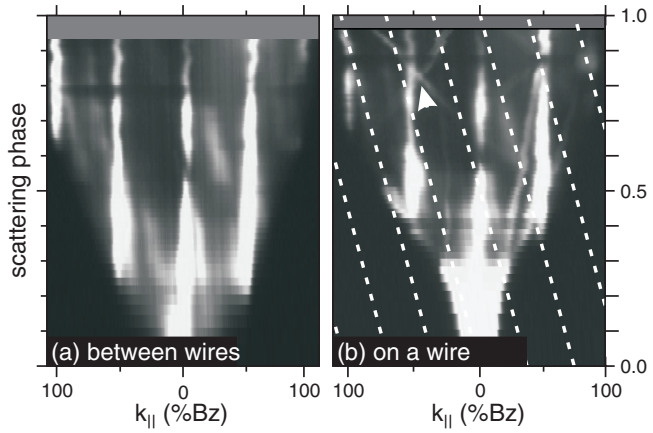

Figure 5. Reciprocal space maps (a) of a surface area between wires exhibiting Si lattice rods, (2 × 3)Ag lattice rods, and (115) facets, and (b) of a wire with surrounding area. Additional facet rods, attributed to the Ag wire, are visible in (b) in addition to the rods of (a).

much weaker, is still present in figure 5(b), and has been marked by parallel lines. All remaining facet spots that have not been marked in (b) are attributed to the side facets of the wire. The presence of wire lattice rods that are slanted to both the left and the right is an indication of the triangular shape of the wire. This particular wire has only one left side facet, while the right side of the wire displays two side facets. Different wires, however, can have different side facets, and a statistical analysis of the side facets of the wires with scanning electron microscopy has yet to be done. In contrast, all wires share the common feature that their facet rods do not intersect on the Si lattice rods (see the arrow in figure 5(b)). This suggests that the Ag nanowire grows with its own lattice constant, in good agreement with the conclusions from TEM [2], mentioned earlier, that there is little strain in the system.

We believe that the step-bunches act as a barrier to surface diffusion in the direction perpendicular to the wire. Thus, diffusion into the sides of the wire is blocked by the step-bunches, and the high temperature is sufficient for the 'slow' diffusion along the steps to supply the ends of the wire with sufficient adatoms to continuously increase the wire's length.

In conclusion, we have studied the growth of Ag nanowires at high temperature on vicinal Si(001), miscut 4° in the [110] direction. The wires grow preferentially along the step edges of the vicinal surface. The length of the wires increases while their width remains constant during deposition as observed in LEEM and PEEM. The length can be controlled during growth, and we have observed the length of some wires increase to more than 100 μm. The crystalline Ag wires appear to be unstrained, and grow with their own lattice constant. We have directly imaged the Ag adatom diffusion fields (iso-coverage zones) surrounding the Ag islands during desorption. This is the first time a diffusion field has been directly imaged in PEEM. The observed iso-coverage zones for both compact and wire-like Ag islands display a striking anisotropy that suggests the presence of a kinetically limiting mechanism that likely contributes to the growth of the wires. We identify this kinetically limiting mechanism as suppressed surface diffusion into the sides of the wires due to adsorbate induced step-bunching, and for the first time the method of reciprocal space mapping has been applied to microdiffraction and LEEM. Since the compact islands also display the anisotropic shape for the iso-coverage zones, there may be some other yet unidentified process contributing to the wires' formation and growth. This further contributing mechanism must also be present to account, for example,

for the formation of the wire-like islands on flat Si(001), as observed in [1] in the absence of step-bunches. It is clear that more detailed studies of the growth of these wire-like islands is necessary to form a universal theoretical understanding of the reasons behind their formation.

Acknowledgments

The authors acknowledge financial support for this research project by the Deutsche Forschungsgemeinschaft in the Sonderforschungsbereich 616: Energy Dissipation at Surfaces. KRR acknowledges support from the National Science Foundation, grant numbers DMR-0203097 and DMR-0320908, and is a Cottrell Scholar of the Research Corporation.

References

[1] Tersoff J and Tromp R M 1993 *Phys. Rev. Lett.* **70** 2782
[2] Swiech W and Zuo J-M 2004 private communication, at press
[3] Jalochowski M and Bauer E 2001 *Surf. Sci.* **480** 109
[4] Jalochowski M and Bauer E 2001 *Prog. Surf. Sci.* **67** 79
[5] Hild R, Meyer zu Heringdorf F-J, Zahl P and Horn-von Hoegen M 2000 *Surf. Sci.* **454–456** 851–5
[6] Horn-von Hoegen M, Minoda H, Yagi K, Meyer zu Heringdorf F-J and Kähler D 1998 *Surf. Sci.* **402–404** 464
[7] Minoda H, Yagi K, Meyer zu Heringdorf F-J, Meier A, Kähler D and Horn-von Hoegen M 1999 *Phys. Rev.* B **59** 2363
[8] Meyer zu Heringdorf F-J, Schmidt Th, Heun S, Hild R, Zahl P, Ressel B, Bauer E and Horn-von Hoegen M 2001 *Phys. Rev. Lett.* **86** 5088
[9] Roos K R, Roos K L, Horn-von Hoegen M and Meyer zu Heringdorf F-J 2004 at press
[10] Tromp R M and Reuter M C 1991 *Ultramicroscopy* **36** 99
[11] Raynerd G, Hardiman M and Venables J A 1991 *Phys. Rev.* B **44** 13803
[12] Chadi D J 1987 *Phys. Rev. Lett.* **59** 1691
[13] Wasserfall J and Ranke W 1994 *Surf. Sci.* **315** 237
[14] Michely T, Reuter M C, Copel M and Tromp R M 1994 *Phys. Rev. Lett.* **73** 2095
[15] Lin X F, Wan K J and Nogami J 1994 *Phys. Rev.* B **49** 7385
[16] Brune H, Bales G S, Jacobsen J, Boragno C and Kern K 1999 *Phys. Rev.* B **60** 5991
[17] See Lifshitz V G, Saranin A A and Zotov A V 1994 *Surface Phases on Silicon* (Chichester: Wiley) and references therein
[18] Zoethout E, Gürlü O, Zandvliet H J W and Poelsema B 2000 *Surf. Sci.* **452** 247
[19] Myslivecek J, Schelling C, Schäffler F, Springholz G, Smilauer P, Krug J and Voigtländer B 2002 *Surf. Sci.* **520** 193
[20] Meier A, Zahl P, Vockenroth R and Horn-von Hoegen M 1998 *Appl. Surf. Sci.* **123/124** 694
[21] Horn-von Hoegen M 1999 *Z. Kristallogr.* **214** 1
[22] Meyer zu Heringdorf F-J and Horn-von Hoegen M 2004 *Rev. Sci. Instrum.* submitted